MOX–Report No. 35/2013

Stabilized extended finite elements for the approximation of saddle point problems with unfitted interfaces

Cattaneo, L.; Formaggia, L.; Iori G. F.; Scotti, A,; Zunino, P.

MOX, Dipartimento di Matematica "F. Brioschi"
Politecnico di Milano, Via Bonardi 9 - 20133 Milano (Italy)

mox@mate.polimi.it http://mox.polimi.it

Stabilized extended finite elements for the approximation of saddle point problems with unfitted interfaces

Laura Cattaneo[♯], Luca Formaggia[♯], Guido Francesco Iori[♯], Anna Scotti[♯]
Paolo Zunino[♯,†]

July 17, 2013

[♯] MOX– Modellistica e Calcolo Scientifico
Dipartimento di Matematica "F. Brioschi"
Politecnico di Milano
via Bonardi 9, 20133 Milano, Italy

[†] Department of Mechanical Engineering and Materials Science
University of Pittsburgh
3700 O'Hara Street, Pittsburgh, PA 15261, USA

Keywords: XFEM, unfitted interface methods, saddle point problems, condition numbers.
AMS Subject Classification: 65N30, 65N12.

Abstract

We address a two-phase Stokes problem, namely the coupling of two fluids with different kinematic viscosities. The domain is crossed by an interface corresponding to the surface separating the two fluids. We observe that the interface conditions allow the pressure and the velocity gradients to be discontinuous across the interface. The eXtended Finite Element Method is applied to accommodate the weak discontinuity of the velocity field across the interface and the jump in pressure on computational meshes that do not fit the interface. Numerical evidence shows that the discrete pressure approximation may be unstable in the neighborhood of the interface, even though the spatial approximation is based on *inf-sup* stable finite elements. It means that XFEM enrichment locally violates the satisfaction of the stability condition for mixed problems. For this reason, resorting to pressure stabilization techniques in the region of elements cut by the unfitted interface is mandatory. In alternative, we consider the application of stabilized equal order pressure / velocity XFEM discretizations and we analyze their approximation properties. On one side, this strategy increases the flexibility on the choice of velocity and pressure approximation spaces. On the other side, symmetric pressure stabilization operators, such as local pressure projection methods or the Brezzi-Pitkaranta scheme, seem to be effective to cure the additional source of instability arising from the XFEM approximation. We will show that these operators can be applied either

locally, namely only in proximity of the interface, or *globally*, that is on the whole domain when combined with equal order approximations. After analyzing the stability, approximation properties and the conditioning of the scheme, numerical results on benchmark cases will be discussed, in order to thoroughly compare the performance of different variants of the method.

1 Introduction and problem set up

Extended finite element methods (XFEMs) represent a vivid subject of research in the field of computational mechanics [20, 12]. The aim of XFEMs is to enable the accurate approximation of problems whose solutions involve jumps, kinks, singularities and other locally non-smooth features within elements. This is achieved by enriching the polynomial approximation space of the classical finite element method with non-smooth functions that resemble the true solution near interfaces. Such methods have shown their potential in several applications of solid mechanics, such as the finite element analysis of cracks, shear bands, dislocations, solidification, and multi-field problems.

Recently, XFEM has been applied to flow problems with moving interfaces, such as the numerical simulation of flows involving immiscible fluids, see for example [14] for a broad introduction or [21] more specific applications. In this context, different types of enrichment strategies for the finite element approximation spaces have been proposed. The method originally proposed in [16] for the approximation of the Laplace equation with contrast coefficients is particularly effective, owing to the good approximation properties and the simplicity of implementation. Indeed, it has been successfully extended to the approximation of saddle point problems in [3, 2, 7, 17]. The main drawback of the method consists in the lack of robustness when the interface cuts the mesh in a way that very small sub-elements are created. Stabilization methods based on the interior penalty approach have been proposed to override this issue [8, 3]. As it will be confirmed by the numerical experiments reported below, for saddle point problems, additional instabilities arise because the enrichment of the Lagrange multiplier space (the pressure) affects the satisfaction of the *inf-sup* condition [4]. There are two possible solutions of this issue. On one hand, the enrichment method could be modified. This strategy has been investigated in a series of works [2, 22, 9]. It seems to be a promising method. However, a complete stability analysis of the propesed approximation spaces is not available yet. On the other hand, the stabilization methods developed to cure the instabilities with respect to small cut-elements may also help to stabilize the pressure. This is the approach successfully adopted in [3, 17].

We aim to investigate the application of XFEMs, in particular of the method proposed in [16], to the approximation of saddle point problems. This method combines weak enforcement of interface conditions using Nitsche's method with XFEM approximation spaces. From now on, we will refer to this family of methods as the Nitsche-XFEM schemes, as proposed in [14]. In particular, we focus our attention on Stokes equations and the related applications. Given a bounded domain $\Omega \subset \mathbb{R}^2$ crossed by an interface Γ dividing Ω into two open sets

Ω_1 and Ω_2 we solve:

$$\begin{cases} -\nabla\cdot(\mu_i\nabla\mathbf{u})+\nabla p=\mathbf{f} & \text{in } \Omega_i, \\ \nabla\cdot\mathbf{u}=0 & \text{in } \Omega_i, \\ \mathbf{u}=0 & \text{on } \partial\Omega, \\ [\![\mathbf{u}]\!]=0 & \text{on } \Gamma, \\ [\![p\mathbf{n}-\mu\nabla\mathbf{u}\cdot\mathbf{n}]\!]=0 & \text{on } \Gamma. \end{cases} \tag{1}$$

The parameter μ_i plays the role of fluid viscosity and is constant in each subdomain Ω_i. Here, since $\mu_1 \neq \mu_2$, the continuity of stresses across Γ induces a kink on the velocity field and a strong discontinuity on pressure (also called jump discontinuity). This is a consequence of the interface conditions $(1)_{d,e}$ where $[\![v]\!] = v|_{\Omega_1} - v|_{\Omega_2}$ denotes the jump across Γ. Accordingly, $\mathbf{n}$ is the unit normal vector on Γ pointing from Ω_1 to Ω_2. Similar issues arise even in the homogeneous case (same parameters in the sub-domains) when a surface tension balancing the jump of the normal stress on the interface is considered, see for example [15].

An approach based on finite elements where the computational mesh does not fit to the interface is not suitable for these kind of problems, because it does not satisfy optimal approximation properties. To preserve accuracy, the strong or weak discontinuities in the solution must coincide with mesh edges. However, for many time-dependent problems such as two-phase flows or fluid-structure interaction, non-matching grid formulations become an interesting option because they avoid remeshing [21, 23, 24].

Mixed finite elements are a typical choice of approximation spaces for the discrete formulation of a saddle point problem without interface. It would be natural to expect that the same of finite element spaces would be adequate to solve the interface problem using the Nitsche-XFEM formulation. The numerical experiment shown in Figure 1 reveals that XFEM spaces do not inherit the *inf-sup* stability of the underlying FEM approximation. More precisely, Figure 1 suggests that pressure oscillations, resembling to the checkerboard instability, appear in the neighborhood of the interface. In this case, the Nitsche-XFEM formulation is applied to solve problem (1) on a quasi uniform mesh cut by a circular interface separating two regions characterized by heterogeneous viscosities. Following the approach already adopted in [3, 17], we investigate how to avoid these oscillations by the choice of suitable enriched finite element spaces and stabilization terms. However, instead of stabilization techniques based on the interior penalty technique, we study behavior of the well known Brezzi-Pitkaranta stabilization technique [5] applied to this new context. Finally, we address the properties of the algebraic system of equations arising from the proposed discretization method. In particular, we study the spectrum of the pressure matrix, showing that the stabilization method is essential to ensure that the conditioning of the system does not depend on the size of cut-elements. This result has an important consequence. It confirms that the classical solution methods for algebraic saddle point problems, such as the Uzawa method, can be successfully combined with this approximation scheme.

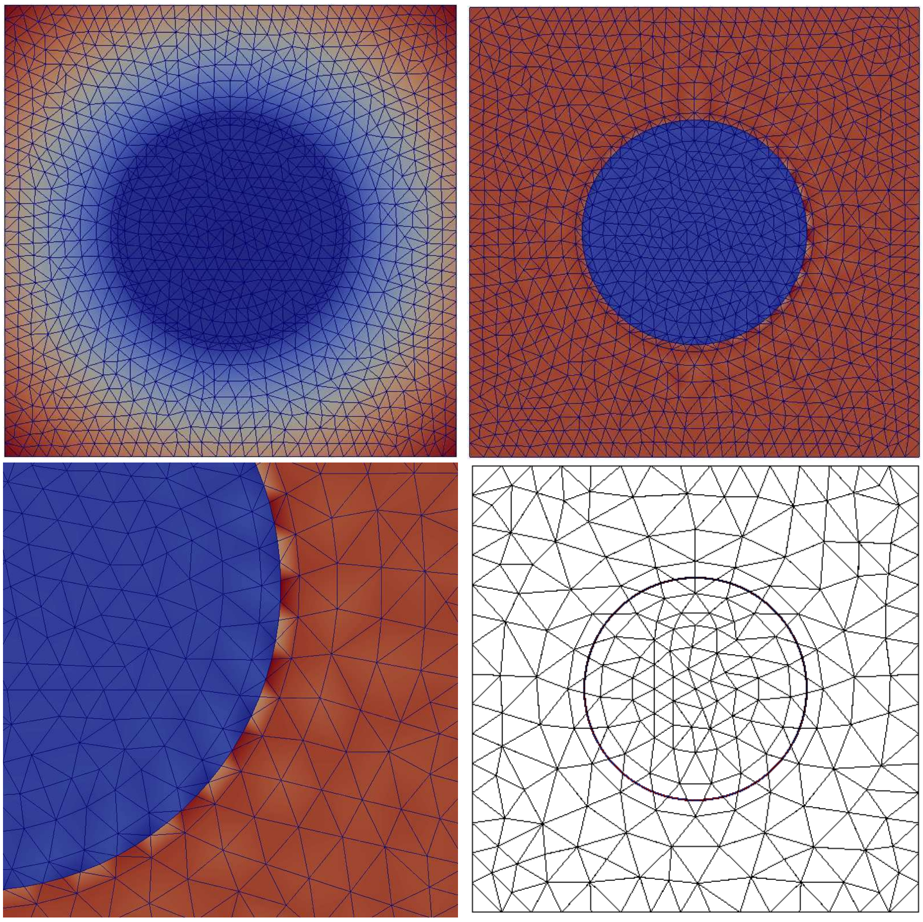

Figure 1: Typical checkerboard pattern of instabilities for the pressure in the cut region (b), while velocity approximation is not affected by instabilities (a). In picture (c), a zoom on the pressure instabilities and in picture (d) the mesh that has been used for testing the conditioning of the problem, which results are reported in Section 4

2 Finite element formulation

We solve (1) on a conforming triangulation $\mathcal{T}_h$ of Ω which is independent of the location of the interface Γ. However, we need to make some assumption concerning the intersection between Γ and the mesh. Let us define the subset of cut elements $\mathcal{G}_h = \{K \in \mathcal{T}_h \text{ such that } K \cap \Gamma \neq \emptyset\}$. In the following, we call this subset of elements *cut region*. Moreover, let us define the triangulated extended and restricted sub-domains, Ω_i^-, Ω_i^+, respectively, with $\Omega_i^- \subset \Omega_i^+$ as follows

$$\Omega_i^+ = \{\mathbf{x} \in K, \forall K \text{ such that } K \cap \Omega_i \neq \emptyset\}, \quad \Omega_i^- = \{\mathbf{x} \in K, \forall K \text{ such that } K \subset \Omega_i\}.$$

We make the following assumptions:

Assumption 1. *For any element K in the cut region and $i = 1, 2$ there exists a patch formed by the union of the element K with some of the elements of Ω_i^- sharing with it an edge (see Figure 2a). This collection of elements is called a macro-element of K and it is denoted with $M_{K,i}$. Furthermore, we assume* *that the restriction of each macro-element to Ω_i^- is not empty, namely $M_{K,i}^- := M_{K,i} \cap \Omega_i^- \neq \emptyset$. Finally, we observe that $M_{K,i}^-$ is at least an element of $\mathcal{T}_h$, such that $|M_{K,i}|/|M_{K,i}^-|$ is always upper bounded.*

Assumption 2. *Γ intersects each element boundary ∂K exactly twice, and each (open) edge at most once.*

Assumption 3. *The interface is defined by the zero isoline of a level set function; the level set function is then approximated by linear interpolation on the computational mesh. The interface is thus represented by a chain of straight segments. We assume that the straight line segment $\Gamma_{K,h}$ connecting the points of intersection between Γ and ∂K is a good approximation of $\Gamma_K = \Gamma \cap K$ in a sense that is detailed in [16]. This construction can be generalized to three space dimensions.*

The first assumption is satisfied if the mesh is uniform, at least in the region neighboring the interface Γ. The last two hypotheses imply that the discrete approximation of the interface subdivides elements into simple shapes (a triangle and a quadrilateral or a couple of triangles).

We can now define the *extended cut region* $\mathcal{S}_h$ as the union of $\mathcal{G}_h$ and all the elements $K \in \mathcal{T}_h$ sharing an edge with at least a cut element (see Figure 2b). This is equivalent to define $\mathcal{S}_h$ as the set of all the elements contained in at least one macro-element for all $K \in \mathcal{G}_h$:

$$\mathcal{S}_h := \bigcup_{K \in \mathcal{G}_h} \bigcup_{i=1,2} M_{K,i}$$

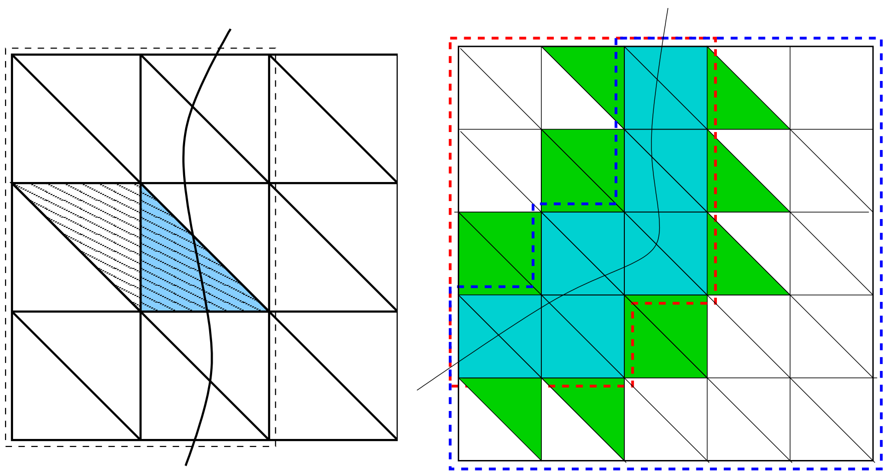

Figure 2: (a) Filled with the diagonal line pattern, a macro-element for an element $K \in \mathcal{G}_h$ (in light blue). This macro-pattern is composed by K, one of its adjacent elements and two other elements sharing a node with it. (b) Definition of Ω_i^+, in light blue the set $\mathcal{G}_h$ and in green the *extended cut region* $\mathcal{S}_h$. As we can see, the extended region contains all the elements near to the cut region, meaning that they share a node or an edge with at least one cut element.

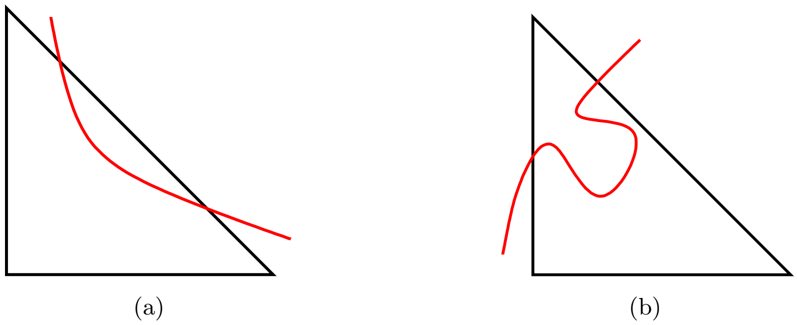

Figure 3: Second (a) and third (b) assumption about the intersection between Γ and $\mathcal{T}_h$ are not satisfied.

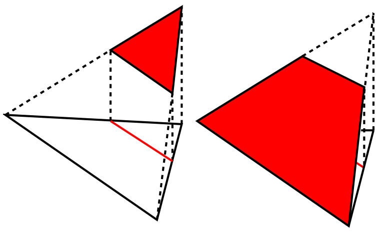

Figure 4: Linear basis function in an element crossed by Γ. The local basis functions ϕ on a cut element K must be discontinuous across Γ:

$$\phi = \begin{cases} \phi_1 \text{ in } K_1 = K \cap \Omega_1 \\ \phi_2 \text{ in } K_2 = K \cap \Omega_2. \end{cases}$$

Since ϕ_1 and ϕ_2 must be independent, we need to double the degrees of freedom on K so that ϕ_1 can be represented in K_1 by its nodal values and the same holds for ϕ_2.

The proposed XFEM method doubles the degrees of freedom in the elements that are crossed by the discontinuity interface, as shown in Figure 4. This is achieved by a suitable definition of the approximation spaces. Let $\mathcal{T}_{h,i}^+$ be conforming triangulations of Ω_i^+ such that the union of $\mathcal{T}_{h,1}^+$ and $\mathcal{T}_{h,2}^+$ gives $\mathcal{T}_h$ and for every triangle $K \in \mathcal{T}_{h,1}^+ \cap \mathcal{T}_{h,2}^+$ we have $K \cap \Gamma \neq \emptyset$. Moreover, we define $\mathcal{T}_{h,i}^- = \mathcal{T}_{h,i}^+ \setminus \mathcal{G}_h$. Let us define the following couple of *inf-sup* stable spaces on the restricted sub-domains Ω_i^-

$$V_{h,i}^- := [\{\phi_h \in C^0(\Omega_i^-), \text{ such that } \phi_h|_K \in \mathbb{P}^1, \forall K \in \mathcal{T}_{h,i}^-\} \cap H_0^1(\Omega_i^-) \oplus B_i]^2,$$
$$Q_{h,i}^- := \{\phi_h \in C^0(\Omega_i^-), \text{ such that } \phi_h|_K \in \mathbb{P}^1, \forall K \in \mathcal{T}_{h,i}^-\}$$

where $B_i = \{b \text{ such that } b|_K \in \mathbb{P}^3 \cap H_0^1(K), \forall K \in \mathcal{T}_{h,i}^-\}$. Let $\mathcal{I}_\Gamma = \{1, ..., n\}$ be the set of all vertexes in the *cut region* $\mathcal{G}_h$ and let

$$W_h = \{\phi_h^j \in C^0(\Omega), \text{ such that } \phi_h|_K \in \mathbb{P}^1, \forall K \in \mathcal{T}_h\} \cap H_0^1(\Omega)$$

be a standard linear finite element space on the triangulation $\mathcal{T}_h$ of the domain Ω and let $\{\phi_h^j\}$ be the Lagrangian basis of W_h. We can now define a couple of finite element spaces on the *cut region*:

$$V_h^{cut} := [span\{\phi_h^j \in W_h\}_{j \in \mathcal{I}_\Gamma}]^2, \quad Q_h^{cut} := span\{\phi_h^j \in W_h\}_{j \in \mathcal{I}_\Gamma}$$

The definition of the finite element spaces for the approximation of our problem follows:

$$V_{h,i} := V_{h,i}^- \oplus V_h^{cut}, \quad Q_{h,i} := Q_{h,i}^- \oplus Q_h^{cut}$$

The enrichment of the *cut region* is obtained by overlapping the spaces $V_{h,i}$ and $Q_{h,i}$ in $\mathcal{G}_h$ which entails that the degrees of freedom of the elements $K \in \mathcal{G}_h$ are doubled. We seek $(\mathbf{u}_{h,i}, p_{h,i}) \in V_{h,i} \times Q_{h,i},\ i = 1,2$ such that $\mathbf{u}_h = (\mathbf{u}_{h,1}, \mathbf{u}_{h,2})$ and $p_h = (p_{h,1}, p_{h,2})$ satisfy:

$$\mathcal{B}_h[(\mathbf{u}_h, p_h), (\mathbf{v}_h, q_h)] + s_h(p_h, q_h) = (\mathbf{f}, \mathbf{v}_h)_\Omega\ ,\ \forall (\mathbf{v}_h, q_h) \in V_h \times Q_h \tag{2}$$

where $V_h = V_{h,1} \times V_{h,2}$, $Q_h = Q_{h,1} \times Q_{h,2}$ and

$$\begin{aligned}
\mathcal{B}_h[(\mathbf{u}_h, p_h), (\mathbf{v}_h, q_h)] :=\ & a_h(\mathbf{u}_h, \mathbf{v}_h) + b_h(p_h, \mathbf{v}_h) - b_h(q_h, \mathbf{u}_h) \\
a_h(\mathbf{u}_h, \mathbf{v}_h) :=& \sum_{i=1,2} \int_{\Omega_i} \mu_i \nabla \mathbf{u}_{h,i} \cdot \nabla \mathbf{v}_{h,i} dx - \int_\Gamma \{\!\{\mu \nabla \mathbf{u}_h \cdot \mathbf{n}\}\!\} [\![\mathbf{v}_h]\!]\, ds \\
& - \int_\Gamma \{\!\{\mu \nabla \mathbf{v}_h \cdot \mathbf{n}\}\!\} [\![\mathbf{u}_h]\!]\, ds + \sum_{K \in \mathcal{G}_h} \int_{\Gamma_K} \gamma_u h_K^{-1} \mu_{max} [\![\mathbf{u}_h]\!] [\![\mathbf{v}_h]\!]\, ds \\
b_h(p_h, \mathbf{v}_h) :=& - \sum_{i=1,2} \int_{\Omega_i} p_{h,i} \nabla \cdot \mathbf{v}_{h,i} dx + \int_\Gamma \{\!\{p_h\}\!\} [\![\mathbf{v}_h \cdot \mathbf{n}]\!]\, ds
\end{aligned}$$

where $\mu_{max} = \max_\Omega \mu$ and we have defined the average operator as $\{\!\{v\}\!\}_\Gamma = k_1 v|_{\Omega_1} + k_2 v|_{\Omega_2}$. For each element $K \in \mathcal{G}_h$, it must hold $k_1 + k_2 = 1$. Typical choices are the standard arithmetic average $k_1 = k_2 = 1/2$, the average depending of the measure of cut elements $k_i = |K \cap \Omega_i|/|K|$ or the following definition proposed in [1]:

$$k_i := \frac{|K \cap \Omega_i|/\mu_i}{|K \cap \Omega_1|/\mu_1 + |K \cap \Omega_2|/\mu_2} \tag{3}$$

We remark that in the homogeneous case we have $\mu_1 = \mu_2$, so that the last two definitions coincide. The term $s_h(p_h, q_h)$ is the stabilization operator defined on the cut region. We are interested in analyzing the properties of the Brezzi-Pitkaranta stabilization technique [5] applied to this new context. For this reason, we consider the following operator acting on the pressure approximation near the interface:

$$s_h(p_h, q_h) := \sum_{i=1,2} \sum_{K \in \mathcal{S}_h} \gamma_s \mu_i^{-1} h_K^2 \int_K \nabla p_{h,i} \cdot \nabla q_{h,i} dx \tag{4}$$

where $\mathcal{S}_h$ is the *extended cut region* previously defined. We remark that the integral in 4 is on the entire *cut* element K. This is crucial to prevent a bad conditioning of the algebraic problem. As we have already pointed out, our choice of spaces $V_{h,i}^-$ and $Q_{h,i}^-$ is *inf-sup* stable on the restricted sub-domains. To be more general, we may use an equal-order stabilized velocity/pressure formulation. This results in adding $c_h(p_h, q_h)$ to the discrete problem formulation. Although $c_h(p_h, q_h)$ can be chosen among the family of symmetric stabilization operators, the most natural choice in our case is the Brezzi-Pitkaranta stabilization:

$$c_h(p_h, q_h) := \sum_{i=1,2} c_{h,i}(p_h, q_h), \quad \text{where} \quad c_{h,i}(p_h, q_h) := \sum_{K \in \mathcal{T}_{h,i}^-} \gamma_s \mu_i^{-1} h_K^2 \int_K \nabla p_{h,i} \cdot \nabla q_{h,i} dx.$$

Redefining the finite element spaces

$$\begin{aligned}
V_{h,i}^- &:= [\{\phi_h \in C^0(\Omega_i^-), \text{ such that } \phi_h|_K \in \mathbb{P}^1, \forall K \in \mathcal{T}_{h,i}^-\} \\
Q_{h,i}^- &:= \{\phi_h \in C^0(\Omega_i^-), \text{ such that } \phi_h|_K \in \mathbb{P}^1, \forall K \in \mathcal{T}_{h,i}^-\}
\end{aligned}$$

we aim to find $\mathbf{u}_h = (\mathbf{u}_{h,1}, \mathbf{u}_{h,2}) \in V_h$ and $p_h = (p_{h,1}, p_{h,2}) \in Q_h$ such that

$$\mathcal{B}_h[(\mathbf{u}_h, p_h), (\mathbf{v}_h, q_h)] + c_h(p_h, q_h) + s_h(p_h, q_h) = (\mathbf{f}, \mathbf{v}_h)_\Omega, \ \forall (\mathbf{v}_h, q_h) \in V_h \times Q_h \quad (5)$$

In the forthcoming sections, we will analyze the two proposed variants of the Nitsche-XFEM scheme.

3 Analysis of the scheme

First of all, let us define the following norms on the trace of a function on Γ:

$$\|v\|^2_{1/2,h,\Gamma} := \sum_{K \in \mathcal{G}_h} h_K^{-1} \|v\|^2_{0,\Gamma_K}, \qquad \|v\|^2_{-1/2,h,\Gamma} := \sum_{K \in \mathcal{G}_h} h_K \|v\|^2_{0,\Gamma_K}$$

Then, we introduce the following broken Sobolev spaces: $H^k_b = \{v : v|_{\Omega_i} \in H^k(\Omega_i), i = 1, 2\}$ with the corresponding norms

$$\|\mathbf{v}\|^2_{k,\Omega} := \sum_{i=1,2} \|\mathbf{v}\|^2_{k,\Omega_i}, \quad \|\mathbf{v}\|^2_{k,\Omega,\mu} := \sum_{i=1,2} \|\mu_i^{1/2}\mathbf{v}\|_{k,\Omega_i}, \quad \|q\|^2_{k,\Omega^\pm,\mu} := \sum_{i=1,2} \|\mu_i^{-1/2} q\|_{k,\Omega_i^\pm},$$

$$|||\mathbf{v}|||^2 := \|\mathbf{v}\|^2_{1,\Omega,\mu} + \|\mu_{max}^{1/2} [\![\mathbf{v}]\!]\|^2_{1/2,h,\Gamma} + \|\mu_{max}^{-1/2} \{\!\{\mu \nabla_{\mathbf{n}} \mathbf{v}\}\!\}\|_{-1/2,h,\Gamma},$$

$$\|(\mathbf{v}, q)\|_{\Omega^+}{}^2 := |||\mathbf{v}|||^2 + \|q\|^2_{0,\Omega^+,\mu} + \|\mu_{max}^{-1/2} \{\!\{q\}\!\}\|^2_{-1/2,h,\Gamma}.$$

Let us define $b_{h,i}(p_h, q_h)$ as the restrictions of $b_h(p_h, q_h)$ on the domains Ω_i,

$$b_{h,i}(p_h, q_h) := -\int_{\Omega_i} p_{h,i} \nabla \cdot \mathbf{v}_{h,i} dx,$$

and let us introduce the discrete trace inequality previously reported in [17], that will be necessary for the theoretical analysis,

$$h_k \|v\|^2_{0,\Gamma_K} \le C \|v\|^2_{0,K}. \quad (6)$$

Thanks to this inequality, taking $q_h \in Q_h$, we have,

$$\begin{aligned}
\|\mu_{max}^{-1/2} \{\!\{q\}\!\}\|^2_{-1/2,h,\Gamma} &\le \|\left\{\!\!\left\{\mu^{-1/2} q_h\right\}\!\!\right\}\|^2_{-1/2,h,\Gamma} = \sum_{K \in \mathcal{G}_h} h_K \|\left\{\!\!\left\{\mu^{-1/2} q_h\right\}\!\!\right\}\|^2_{0,\Gamma_K} \\
&\le \sum_{K \in \mathcal{G}_h} h_K (\|\mu_1^{-1/2} k_1 q_{h,1}\|^2_{0,\Gamma_K} + \|\mu_2^{-1/2} k_2 q_{h,2}\|^2_{0,\Gamma_K}) \\
&\le C \sum_{i=1,2} \sum_{K \in \mathcal{G}_h} \|\mu_i^{-1/2} k_i q_{h,i}\|^2_{0,K} \\
&\le C \sum_{i=1,2} \sum_{K \in \mathcal{G}_h} \|\mu_i^{-1/2} q_{h,i}\|^2_{0,K} \\
&\le C \sum_{i=1,2} \sum_{K \in \mathcal{T}^+_{h,i}} \|\mu_i^{-1/2} q_{h,i}\|^2_{0,K} = C \|q_h\|^2_{0,\Omega^+,\mu}.
\end{aligned}$$

In particular, the following discrete norm equivalence holds true,

$$|||\mathbf{v}|||^2 + \|q_h\|^2_{0,\Omega^+,\mu} \le \|(\mathbf{v}, q_h)\|_{\Omega^+}{}^2 \le |||\mathbf{v}|||^2 + (1 + C) \|q_h\|^2_{0,\Omega^+,\mu}. \quad (7)$$

3.1 Stability analysis

The first part of our theoretical analysis focuses on the stability of the scheme.

Theorem 3.1. *We assume that our finite element scheme is inf-sup stable away from the cut region. More precisely, from now on the following assumption holds true: there exist constants C_{p1} and C_{p2}, independent on the mesh size, such that $\forall p_{h,i} \in Q_{h,i}$ there exists $\mathbf{v}_{p_{h,i}} \in V_{h,i} \cap H^1_0(\Omega_i^-)$,*

$$\|\mathbf{v}_{p_{h,i}}\|_{1,\Omega_i^-,\mu} \leq C_{p1}\|p_{h,i}\|_{0,\Omega_i^-,\mu}, \tag{8}$$

$$C_{p2}\|p_{h,i}\|_{0,\Omega_i^-,\mu} \leq b_{h,i}(p_{h,i}, \mathbf{v}_{p_{h,i}}) + c_{h,i}(p_{h,i}, p_{h,i}). \tag{9}$$

Under these assumptions, there exists a positive constant c, independent on the mesh characteristic size such that, for any $(\mathbf{u}_h, p_h) \in V_h \times Q_h$ it holds:

$$C_s\|(\mathbf{u}_h, p_h)\|_{\Omega^+} \leq \sup_{(\mathbf{v}_h,q_h)\in V_h\times Q_h} \frac{\mathcal{B}_h[(\mathbf{u}_h, p_h), (\mathbf{v}_h, q_h)] + c_h(p_h, q_h) + s_h(p_h, q_h)}{\|(\mathbf{v}_h, q_h)\|_{\Omega^+}}. \tag{10}$$

We remark that (8) implies

$$\|\mathbf{v}_{p_{h,i}}\|_{1,\Omega_i^-,\mu} \leq C_{p1}\|p_{h,i}\|_{0,\Omega_i^+,\mu}.$$

To prove (10), we start showing the properties of the bilinear forms $a_h(\mathbf{u}_h, \mathbf{v}_h)$, $b_h(\mathbf{v}_h, p_h)$, $c_h(p_h, q_h)$ and $s_h(p_h, q_h)$.

Lemma 3.2. *The bilinear discrete form $a_h(\mathbf{u}_h, \mathbf{v}_h)$ is continuous on V_h and coercive, provided γ_u is chosen sufficiently large. That is, there exist two constants C_m and C_a, independent on the mesh size such that*

$$a_h(\mathbf{u}_h, \mathbf{v}_h) \leq C_m|||\mathbf{u}_h||| |||\mathbf{v}_h|||, \quad \forall \mathbf{v}_h \in V_h, \tag{11}$$

$$a_h(\mathbf{v}_h, \mathbf{v}_h) \geq C_a|||\mathbf{v}_h|||^2, \quad \forall \mathbf{v}_h \in V_h. \tag{12}$$

Let $\mathbf{v}_h \in V_h$, $p_h \in Q_h$ and $q_h \in Q_h$. There exist three constants C_b, C_{s1} and C_{s2}, independent on the mesh size, such that

$$b_h(\mathbf{v}_h, p_h) \leq C_b|||\mathbf{v}_h|||(\|p_h\|_{0,\Omega^+,\mu} + \|\mu_{max}^{-1/2}\{\!\{p_h\}\!\}\|^2_{-1/2,h,\Gamma}) \tag{13}$$

$$c_h(p_h, q_h) \leq C_{s1}\|p_h\|_{0,\Omega^+,\mu}\|q_h\|_{0,\Omega^+,\mu}, \tag{14}$$

$$s_h(p_h, q_h) \leq C_{s2}\|p_h\|_{0,\Omega^+,\mu}\|q_h\|_{0,\Omega^+,\mu}. \tag{15}$$

Furthermore, owing to (11) and (13), the bilinear discrete form $\mathcal{B}_h[(\mathbf{u}_h, p_h), (\mathbf{v}_h, q_h)]$ is continuous on $V_h \times Q_h$,

$$\mathcal{B}_h[(\mathbf{u}_h, p_h), (\mathbf{v}_h, q_h)] \leq C_B\|(\mathbf{u}_h, p_h)\|_{\Omega^+}\|(\mathbf{v}_h, q_h)\|_{\Omega^+}. \tag{16}$$

Proof. To prove (12), we use the following generalized inverse estimate,

$$\|\{\!\{\mu\nabla_{\mathbf{n}}\mathbf{v}_h\}\!\}\|^2_{-1/2,h,\Gamma} \leq C_I\mu_{max}\|\mathbf{v}_h\|^2_{1,\Omega,\mu} \tag{17}$$

that highlights the role of the weights k_i defined in (3), required to obtain a robust form of the Nitsche's method. In particular, since $\mathbf{v}_h$ is linear in $\mathcal{G}_h$, for every $K \in \mathcal{G}_h$ we have,

$$
\begin{aligned}
\|\{\!\{\mu\nabla_{\mathbf{n}}\mathbf{v}_h\}\!\}\|^2_{-1/2,h,\Gamma_K} &= h_K|\Gamma_K|\left(k_1\mu_1\nabla_{\mathbf{n}}\mathbf{v}_{h,1} + k_2\mu_2\nabla_{\mathbf{n}}\mathbf{v}_{h,2}\right)^2 \\
&\leq h_K \sum_{i=1,2} \frac{|\Gamma_K|}{|K\cap\Omega_i|} k_i^2\mu_i^2\|\nabla\mathbf{v}_{h,i}\|^2_{0,K\cap\Omega_i} \\
&= h_K \sum_{i=1,2} \frac{|\Gamma_K|}{|K\cap\Omega_i|} \frac{|K\cap\Omega_i|^2/\mu_i^2}{\left(\sum\limits_{j=1,2}|K\cap\Omega_j|/\mu_j\right)^2}\mu_i^2\|\nabla\mathbf{v}_{h,i}\|^2_{0,K\cap\Omega_i} \\
&= h_K|\Gamma_K|\frac{1}{\left(\sum\limits_{j=1,2}|K\cap\Omega_j|/\mu_j\right)^2}\sum_{i=1,2}\frac{|K\cap\Omega_i|}{\mu_i}\|\mu_i^{1/2}\nabla\mathbf{v}_{h,i}\|^2_{0,K\cap\Omega_i} \\
&\leq h_K|\Gamma_K|\frac{1}{|K\cap\Omega_1|/\mu_1 + |K\cap\Omega_2|/\mu_2}\sum_{i=1,2}\|\nabla\mathbf{v}_{h,i}\|^2_{0,K\cap\Omega_i,\mu} \\
&\leq \frac{h_K|\Gamma_K|}{|K|}\mu_{max}\|\nabla\mathbf{v}_h\|^2_{0,K,\mu} \\
&= C_{I,K}\mu_{max}\|\nabla\mathbf{v}_h\|^2_{0,K,\mu}.
\end{aligned}
$$

Summing over all the elements K $\in \mathcal{G}_h$ and setting $C_I = \max\limits_K C_{I,K}$ we have

$$
\begin{aligned}
\|\{\!\{\mu\nabla_{\mathbf{n}}\mathbf{v}_h\}\!\}\|^2_{-1/2,h,\Gamma} &\leq \sum_{K\in\mathcal{G}_h} C_{I,K}\mu_{max}\|\nabla\mathbf{v}_h\|^2_{0,K,\mu} \\
&\leq C_I\mu_{max}\sum_{K\in\mathcal{T}_h}\|\nabla\mathbf{v}_h\|^2_{0,K,\mu} \\
&= C_I\mu_{max}\|\nabla\mathbf{v}_h\|^2_{0,\Omega,\mu}.
\end{aligned}
$$

We are now ready to prove coercivity.

$$
\begin{aligned}
a_h(\mathbf{v}_h,\mathbf{v}_h) &= \sum_{i=1,2}\int_\Omega \mu_i(\nabla\mathbf{v}_{h,i})^2dx - 2\int_\Gamma [\![\mathbf{v}_h]\!]\,\{\!\{\mu\nabla_{\mathbf{n}}\mathbf{v}_h\}\!\}\,ds + \int_\Gamma \gamma_u\mu_{max}h_K^{-1}([\![\mathbf{v}_h]\!])^2ds \\
&\geq \|\mathbf{v}_h\|^2_{1,\Omega,\mu} + \gamma_u\|\mu_{max}^{1/2}[\![\mathbf{v}_h]\!]\|^2_{1/2,h,\Gamma} - 2\|\mu_{max}^{1/2}[\![\mathbf{v}_h]\!]\|_{1/2,h,\Gamma}\|\mu_{max}^{-1/2}\{\!\{\mu\nabla_{\mathbf{n}}\mathbf{v}_h\}\!\}\|_{-1/2,h,\Gamma} \\
&\geq \|\mathbf{v}_h\|^2_{1,\Omega,\mu} + (\gamma_u-\epsilon)\|\mu_{max}^{1/2}[\![\mathbf{v}_h]\!]\|^2_{1/2,h,\Gamma} - \frac{1}{\epsilon}\|\mu_{max}^{-1/2}\{\!\{\mu\nabla_{\mathbf{n}}\mathbf{v}_h\}\!\}\|^2_{-1/2,h,\Gamma}.
\end{aligned}
$$

Then, it follows form (17) that

$$
\begin{aligned}
a_h(\mathbf{v}_h,\mathbf{v}_h) &\geq \frac{1}{2}\|\mathbf{v}_h\|^2_{1,\Omega,\mu} + \left(\frac{1}{2}-\frac{2C_I}{\epsilon}\right)\|\mathbf{v}_h\|^2_{1,\Omega,\mu} \\
&\quad + \frac{1}{\epsilon}\|\mu_{max}^{-1/2}\{\!\{\mu\nabla_{\mathbf{n}}\mathbf{v}_h\}\!\}\|^2_{-1/2,h,\Gamma} + (\gamma_u-\epsilon)\|\mu_{max}^{1/2}[\![\mathbf{v}_h]\!]\|^2_{1/2,h,\Gamma}.
\end{aligned}
$$

Taking $\epsilon = 4C_I$ and choosing $\gamma_u > 4C_I$ the coercivity of $a_h(\mathbf{u}_h,\mathbf{v}_h)$ follows, since

$$
a_h(\mathbf{v}_h,\mathbf{v}_h) \geq \min\{\frac{1}{2}, C_{\gamma_u}, \frac{1}{4C_I}\}(\|\mathbf{v}_h\|^2_{1,\Omega,\mu} + \|\mu_{max}^{1/2}[\![\mathbf{v}_h]\!]\|^2_{1/2,h,\Gamma} + \|\mu_{max}^{-1/2}\{\!\{\mu\nabla_{\mathbf{n}}\mathbf{v}_h\}\!\}\|^2_{-1/2,h,\Gamma})
$$

where $C_{\gamma_u} = (\gamma_u - 4C_I)$. This completes the proof. Continuity of the discrete form $a_h(\mathbf{u}_h,\mathbf{v}_h)$ follows directly from its definition, while to prove the continuity of $b_h(p_h, \mathbf{v}_h)$ we proceed as follows,

$$\begin{aligned}
b_h(p_h, \mathbf{v}_h) &= -\sum_{i=1,2} \int_{\Omega_i} p_{h,i} \nabla \cdot \mathbf{v}_{h,i} dx + \int_\Gamma \{\!\{p_h\}\!\} [\![\mathbf{v}_h \cdot \mathbf{n}]\!] \, ds \\
&\le \|p_h\|_{0,\Omega^+,\mu} \|v_h\|_{1,\Omega,\mu} + \|\mu_{max}^{-1/2} \{\!\{p_h\}\!\}\|_{-1/2,h,\Gamma} \|\mu_{max}^{1/2} [\![\mathbf{v}_h \cdot \mathbf{n}]\!]\|_{1/2,h,\Gamma} \\
&\le C_b |||\mathbf{v}_h|||(\|p_h\|_{0,\Omega^+,\mu} + \|\mu_{max}^{-1/2} \{\!\{p_h\}\!\}\|_{-1/2,h,\Gamma}).
\end{aligned}$$

Continuity of the stabilization operator $c_h(p_h, q_h)$ is then proved,

$$\begin{aligned}
c_h(p_h, q_h) &= \sum_{i=1,2} \sum_{K \in \mathcal{T}_{h,i}^-} \gamma_s \mu_i^{-1} h_K^2 \int_K \nabla p_{h,i} \cdot \nabla q_{h,i} dx \\
&\le \sum_{i=1,2} \sum_{K \in \mathcal{T}_{h,i}^-} \gamma_s h_K^2 h_K^{-2} \|\mu_i^{-1/2} p_h\|_{0,K} \|\mu_i^{-1/2} q_h\|_{0,K} \\
&\le C_{s1} \|p_h\|_{0,\Omega^+,\mu} \|q_h\|_{0,\Omega^+,\mu}.
\end{aligned}$$

Here the first inequality follows from the inverse inequality. The continuity of $s_h(p_h, q_h)$ is actually obtained in the same way. Summing estimates (11) and (13) and using the definition of the norm $\|(\cdot,\cdot)\|_{\Omega^+}$ yield the result (16). □

To prove the *inf-sup* condition, we first consider a stability estimate for a projection operator.

Lemma 3.3. *The L^2 projection operator on a macro-element $M_{K,i}$, namely $\Pi_h : H^1(M_{K,i}) \mapsto \mathbb{P}^1(M_{K,i})$, satisfies the following property:*

$$\|p_{h,i}\|_{0,\Omega_i^+,\mu}^2 \le C \left(\|p_{h,i}\|_{0,\Omega_i^-,\mu}^2 + \gamma_{h,i}(p_{h,i}, p_{h,i}) \right), \tag{18}$$

where

$$\gamma_{h,i}(p_{h,i}, q_{h,i}) := \sum_{K \in \mathcal{G}_h} \int_{M_{K,i}} \gamma_s \mu_i^{-1} (1-\Pi_h) p_{h,i} (1-\Pi_h) q_{h,i}, \quad \gamma_h(p_h, q_h) := \sum_{i=1,2} \gamma_{h,i}(p_{h,i}, q_{h,i})$$

and C is a constant dependent on the total number of elements that can form a macro-element $M_{K,i}$ with a generic element $K \in \mathcal{G}_h$.

Proof. Since $\Pi_h p_{h,i}$ is a linear function on a macro-element, it holds that:

$$\|\Pi_h p_{h,i}\|_{0,M_{K,i}}^2 \lesssim \frac{|M_{K,i}|}{|M_{K,i}^-|} \|\Pi_h p_{h,i}\|_{0,M_{K,i}^-}^2,$$

where we have introduced the notation $x \lesssim y$ to represent the existence of a generic constant c such that $x \le cy$. We represent $p_{h,i}|_{M_{K,i}}$ as the sum of the linear part and a residual: $p_{h,i}|_{M_{K,i}} = \Pi_h p_{h,i} + r_{h,i}$. It follows that

$$\begin{aligned}
\|p_{h,i}\|_{0,M_{K,i}}^2 &= \|\Pi_h p_{h,i} + r_{h,i}\|_{0,M_{K,i}}^2 \\
&= \|\Pi_h p_{h,i}\|_{0,M_{K,i}}^2 + \|r_{h,i}\|_{0,M_{K,i}}^2 \\
&\lesssim \frac{|M_{K,i}|}{|M_{K,i}^-|} \|\Pi_h p_{h,i}\|_{0,M_{K,i}^-}^2 + \|r_{h,i}\|_{0,M_{K,i}}^2.
\end{aligned}$$

Owing to assumption 1, the ratio between the measure of the entire macro-element and that of its restriction is upper bounded. We now consider the second member of the last inequality, where we identify $\beta = |M_{K,i}|/|M^-_{K,i}|$ in order to simplify the notation:

$$
\begin{aligned}
\beta\|\Pi_h p_{h,i}\|^2_{0,M^-_{K,i}} + \|r_{h,i}\|^2_{0,M_{K,i}} &= \beta\|\Pi_h p_{h,i}\|^2_{0,M^-_{K,i}} + \|r_{h,i}\|^2_{0,M_{K,i}} \pm \beta\|r_{h,i}\|^2_{0,M^-_{K,i}} \\
&\leq \beta \int_{M^-_{K,i}} (\Pi_h p_{h,i} - r_{h,i})(\Pi_h p_{h,i} + r_{h,i}) + (1+\beta)\|r_{h,i}\|^2_{0,M_{K,i}} \\
&\leq \frac{\beta\epsilon}{2}\|\Pi_h p_{h,i} - r_{h,i}\|^2_{0,M_{K,i}} + \frac{\beta}{2\epsilon}\|p_{h,i}\|^2_{0,M^-_{K,i}} + (1+\beta)\|r_{h,i}\|^2_{0,M_{K,i}} \\
&\leq \beta\epsilon\|\Pi_h p_{h,i}\|^2_{0,M_{K,i}} + \beta\epsilon\|r_{h,i}\|^2_{0,M_{K,i}} + \frac{\beta}{2\epsilon}\|p_{h,i}\|^2_{0,M^-_{K,i}} \\
&\quad + (1+\beta)\|r_{h,i}\|^2_{0,M_{K,i}}.
\end{aligned}
$$

Choosing the same ϵ as before, we get

$$
\|p_{h,i}\|^2_{0,M_{K,i}} = (1-\beta\epsilon)\|p_{h,i}\|^2_{0,M_{K,i}} + \beta\epsilon\|\Pi_h p_{h,i}\|^2_{0,M_{K,i}} + \beta\epsilon\|r_{h,i}\|^2_{0,M_{K,i}}.
$$

As a result, we obtain

$$
\begin{aligned}
&(1-\beta\epsilon)\|p_{h,i}\|^2_{0,M_{K,i}} + \beta\epsilon\|\Pi_h p_{h,i}\|^2_{0,M_{K,i}} + \beta\epsilon\|r_{h,i}\|^2_{0,M_{K,i}} \\
&\lesssim \beta\epsilon\|\Pi_h p_{h,i}\|^2_{0,M_{K,i}} + \beta\epsilon\|r_{h,i}\|^2_{0,M_{K,i}} + \frac{\beta}{2\epsilon}\|p_{h,i}\|^2_{0,M^-_{K,i}} + (1+\beta)\|r_{h,i}\|^2_{0,M_{K,i}},
\end{aligned}
$$

from which it follows that

$$
\|p_{h,i}\|^2_{0,M_{K,i}} \lesssim \frac{\beta}{2\epsilon(1-\beta\epsilon)}\|p_{h,i}\|^2_{0,M^-_{K,i}} + \frac{1+\beta}{1-\beta\epsilon}\|r_{h,i}\|^2_{0,M_{K,i}}. \tag{19}
$$

To conclude, we sum over all elements of Ω_i^+ and we rescale all norms using $\mu_i^{-1/2}$,

$$
\begin{aligned}
\|p_{h,i}\|^2_{0,\Omega_i^+,\mu} &= \|p_{h,i}\|^2_{0,\Omega_i^-,\mu} + \sum_{K\in\mathcal{G}_h} \|\mu_i^{-1/2} p_{h,i}\|^2_{0,K} \\
&\leq \|p_{h,i}\|^2_{0,\Omega_i^-,\mu} + \sum_{K\in\mathcal{G}_h} \|\mu_i^{-1/2} p_{h,i}\|^2_{0,M_{K,i}} \\
&\lesssim \|p_{h,i}\|^2_{0,\Omega_i^-,\mu} + \sum_{K\in\mathcal{G}_h} \left(\|\mu_i^{-1/2} p_{h,i}\|^2_{0,M^-_{K,i}} + \|\mu_i^{-1/2} r_{h,i}\|^2_{0,M_{K,i}}\right) \\
&\lesssim C(\mathcal{T}_h)\left(\|p_{h,i}\|^2_{0,\Omega_i^-,\mu} + \gamma_{h,i}(p_{h,i},p_{h,i})\right).
\end{aligned}
$$

We remark that, since we sum on the macro-elements of all $K \in \mathcal{G}_h$, some elements will be counted more than once. The mesh-dependent constant $C(\mathcal{T}_h)$ that appear in the proof takes into account this effect. □

This result gives origin to several families of stabilization methods. Notably the ghost penalty methods as well as the Brezzi-Pitkaranta stabilization can be seen as schemes to control the local operator.

Lemma 3.4. *The stabilization term*

$$s_h(p_h, q_h) = \sum_{i=1,2} \sum_{K \in \mathcal{S}_h} \gamma_s \mu_i^{-1} h_K^2 \int_K \nabla p_{h,i} \cdot \nabla q_{h,i} dx$$

dominates on the local projection stabilization, that is

$$\gamma_h(q_h, q_h) \lesssim s_h(q_h, q_h). \tag{20}$$

Proof. We use the following result [11, 6]:

$$\|q_{h,i} - \Pi_h q_{h,i}\|_{0,M_{K,i}} \le Ch \|\nabla q_{h,i}\|_{L^2(M_{K,i})}, \quad \forall q_{h,i} \in Q_{h,i},$$

where the constant C is independent of the mesh size. We can now write,

$$\begin{aligned}
\gamma_h(q_h, q_h) &= \sum_{i=1,2} \sum_{K \in \mathcal{G}_h} \gamma_s \mu_i^{-1} \|(1 - \Pi_h) q_{h,i}\|^2_{0,M_{K,i}} \\
&\le \sum_{i=1,2} \sum_{K \in \mathcal{G}_h} C \gamma_s \mu_i^{-1} h_K^2 \|\nabla q_{h,i}\|^2_{0,M_{K,i}} \\
&\le C(\mathcal{T}_h) \sum_{i=1,2} \sum_{K \in \mathcal{S}_h} \gamma_s \mu_i^{-1} h_K^2 \|\nabla q_{h,i}\|^2_{0,K} \\
&\lesssim s_h(q_h, q_h).
\end{aligned}$$

□

The following property is a consequence of lemmas 3.3 and 3.4:

$$\|p_{h,i}\|^2_{0,\Omega_i^+,\mu} \lesssim \|p_{h,i}\|^2_{0,\Omega_i^-,\mu} + s_h(p_{h,i}, p_{h,i}). \tag{21}$$

It shows that in the Nitsche-XFEM method, the discrete pressure can be controlled provided that an inf-sup stable velocity/pressure approximation is combined with the Brezzi-Pitkaranta operator restricted to the neighborhood of the cut region. Using standard arguments, see [3], we now prove that the scheme is stable in the sense specified in Theorem 3.1.

of theorem 3.1. As a first step, we prove the *inf-sup* stability on the domain Ω, given the local stability estimates (on the restricted sub-domains):

$$b(p_h, \mathbf{v}_{p_h}) + c_h(p_h, p_h) + s_h(p_h, p_h) \gtrsim C_{p2} \|p_h\|^2_{0,\Omega^+,\mu}. \tag{22}$$

We take a $\mathbf{v}_{p_h} = (\mathbf{v}_{p_{h,1}}, \mathbf{v}_{p_{h,2}})$ satisfying the assumptions of the theorem and, reminding that $\mathbf{v}_{p_{h,i}}$ are null on the *cut region* since their support is limited to the restricted sub-domain Ω_i^-, we can write:

$$b(p_h, \mathbf{v}_{p_h}) = -\sum_{i=1,2} \int_{\Omega_i} p_{h,i} \nabla \cdot \mathbf{v}_{p_{h,i}} dx + \int_\Gamma \{\!\{p_h\}\!\} [\![\mathbf{v}_{p_h} \cdot \mathbf{n}]\!] \, ds = \sum_{i=1,2} b_{h,i}(p_{h,i}, \mathbf{v}_{p_{h,i}})$$

$$\sum_{i=1,2} \big(b_{h,i}(p_{h,i}, \mathbf{v}_{p_{h,i}}) + c_{h,i}(p_{h,i}, q_{h,i}) \big) = b_h(p_h, \mathbf{v}_{p_h}) + c_h(p_h, p_h) \gtrsim \sum_{i=1,2} C_{p2} \|p_{h,i}\|_{0,\Omega_i^-,\mu}.$$

Using inequality (21), we are now able to prove the global *inf-sup* stability (22):

$$\begin{aligned}
b_h(p_h, \mathbf{v}_{p_h}) + c_h(p_h, p_h) + s_h(p_h, p_h) &\ge \sum_{i=1,2} C_{p2} \|p_{h,i}\|_{0,\Omega_i^-,\mu} + s_h(p_h, p_h) \\
&\gtrsim C_{p2} \|p_h\|^2_{0,\Omega^+,\mu}.
\end{aligned}$$

We are now ready to complete the proof. Using the test functions $\mathbf{v}_h = \mathbf{u}_h + \eta \mathbf{v}_{p_h}$ and $q_h = p_h$, we obtain that

$$\begin{aligned}\|(\mathbf{v}_h, q_h)\|_{\Omega^+} &= \|(\mathbf{u}_h + \eta\mathbf{v}_{p_h}, p_h)\|_{\Omega^+} \le \|(\mathbf{u}_h, p_h)\|_{\Omega^+} + \|(\eta\mathbf{v}_{p_h}, 0)\|_{\Omega^+} \\ &= \|(\mathbf{u}_h, p_h)\|_{\Omega^+} + |||\eta\mathbf{v}_{p_h}||| = \|(\mathbf{u}_h, p_h)\|_{\Omega^+} + \|\eta\mathbf{v}_{p_h}\|_{1,\Omega,\mu}\end{aligned}$$

and using (8) we get,

$$\begin{aligned}\|\eta\mathbf{v}_{p_h}\|^2_{1,\Omega,\mu} = \eta^2\|\mathbf{v}_{p_h}\|^2_{1,\Omega,\mu} &\le \eta^2 \sum_{i=1,2} C_{p1}^2 \|p_{h,i}\|^2_{0,\Omega_i^-,\mu} \\ &\le \eta^2 \sum_{i=1,2} C_{p1}^2 \|p_{h,i}\|^2_{0,\Omega_i^+,\mu} \le \eta^2 C_{p1}^2 \|(\mathbf{u}_h, p_h)\|_{\Omega^+}{}^2\end{aligned}$$

which allows us to write,

$$\|(\mathbf{v}_h, q_h)\|_{\Omega^+} \le \|(\mathbf{u}_h, p_h)\|_{\Omega^+} + \eta C_{p1}\|(\mathbf{u}_h, p_h)\|_{\Omega^+} = (1+\eta C_{p1})\|(\mathbf{u}_h, p_h)\|_{\Omega^+} \lesssim \|(\mathbf{u}_h, p_h)\|_{\Omega^+}.$$

Now we develop the term $\mathcal{B}_h[(\mathbf{u}_h, p_h), (\mathbf{v}_h, q_h)]$ as

$$\begin{aligned}\mathcal{B}_h[(\mathbf{u}_h, p_h), (\mathbf{v}_h, q_h)] &= a_h(\mathbf{u}_h, \mathbf{u}_h + \eta\mathbf{v}_{p_h}) + b_h(p_h, \mathbf{u}_h + \eta\mathbf{v}_{p_h}) - b_h(p_h, \mathbf{u}_h) \\ &= a_h(\mathbf{u}_h, \mathbf{u}_h) + a_h(\mathbf{u}_h, \eta\mathbf{v}_{p_h}) + b_h(p_h, \eta\mathbf{v}_{p_h}).\end{aligned} \tag{23}$$

As for the term $a_h(\mathbf{u}_h, \eta\mathbf{v}_{p_h})$, we get

$$\begin{aligned}a_h(\mathbf{u}_h, \eta\mathbf{v}_{p_h}) &= \sum_{i=1,2} \int_{\Omega_i} \mu_i \nabla\mathbf{u}_{h,i} \eta \nabla\mathbf{v}_{p_{h,i}} dx - \int_\Gamma \{\!\{\mu\nabla_{\mathbf{n}}\mathbf{v}_{p_h}\}\!\} [\![\mathbf{u}_h]\!]\, ds \\ &\le \|\mathbf{u}_h\|_{1,\Omega,\mu}\|\eta\mathbf{v}_{p_h}\|_{1,\Omega,\mu} \\ &\le \frac{\epsilon}{2}\|\mathbf{u}_h\|^2_{1,\Omega,\mu} + \frac{1}{2\epsilon}\|\eta\mathbf{v}_{p_h}\|^2_{1,\Omega,\mu} \\ &\le \frac{\epsilon}{2}\|\mathbf{u}_h\|^2_{1,\Omega,\mu} + \frac{C_{p1}\eta^2}{2\epsilon}\|p_h\|^2_{0,\Omega^+,\mu}.\end{aligned} \tag{24}$$

Using (12), (22), (24) and the norm equivalence (7) we obtain

$$\begin{aligned}&\mathcal{B}_h[(\mathbf{u}_h, p_h), (\mathbf{v}_h, q_h)] + c_h(p_h, q_h) + s_h(p_h, q_h) \\ &\quad \ge C_a|||\mathbf{u}_h|||^2 - \frac{\epsilon}{2}\|\mathbf{u}_h\|^2_{1,\Omega,\mu} - \frac{C_{p1}\eta^2}{2\epsilon}\|p_h\|^2_{0,\Omega^+,\mu} + C_{p2}\|p_h\|^2_{0,\Omega^+,\mu} \\ &\quad \ge (C_a - \frac{\epsilon}{2})|||\mathbf{u}_h|||^2 + (C_{p2} - \frac{C_{p1}\eta^2}{2\epsilon})\|p_h\|^2_{0,\Omega^+,\mu} \ge C_s\|(\mathbf{u}_h, p_h)\|_{\Omega^+}{}^2,\end{aligned}$$

and dividing by $\|(\mathbf{v}_h, q_h)\|_{\Omega^+}$ we have:

$$\begin{aligned}\frac{\mathcal{B}_h[(\mathbf{u}_h, p_h), (\mathbf{v}_h, q_h)] + c_h(p_h, q_h) + s_h(p_h, q_h)}{\|(\mathbf{v}_h, q_h)\|_{\Omega^+}} &\ge \frac{\mathcal{B}_h[(\mathbf{u}_h, p_h), (\mathbf{v}_h, q_h)] + c_h(p_h, q_h) + s_h(p_h, q_h)}{\|(\mathbf{u}_h, p_h)\|_{\Omega^+}} \\ &\ge C_s\|(\mathbf{u}_h, p_h)\|_{\Omega^+}.\end{aligned}$$

The thesis (10) of the theorem holds by choosing ϵ and η such that

$$\epsilon < 2C_a \quad \text{and} \quad \eta < \sqrt{\frac{2C_{p2}\epsilon}{C_{p1}}}.$$

$\square$

3.2 Error analysis

We start from the consistency of the scheme which will be useful in the derivation of the error estimate. For the derivation we follow [16] and [3].

Lemma 3.5. *Let* $(\mathbf{u}_h, p_h)$ *be the solution of the finite element formulation* (2) *and* $(\mathbf{u}, p) \in [H^2(\Omega_1 \cup \Omega_2)]^2 \times H^1(\Omega_1 \cup \Omega_2)$ *be the weak solution of* (1)*. Then the finite element formulation* (2) *fulfills the following consistency relation,*

$$\mathcal{B}_h[(\mathbf{u}-\mathbf{u}_h, p-p_h), (\mathbf{v}_h, q_h)] = c_h(p_h, q_h) + s_h(p_h, q_h),\ \forall (\mathbf{v}_h, q_h) \in V_h \times Q_h. \quad (25)$$

Proof. The property follows observing that the exact solution $(\mathbf{u}, p)$ satisfies

$$\mathcal{B}_h[(\mathbf{u}, p), (\mathbf{v}_h, q_h)] = (\mathbf{f}, \mathbf{v}_h)_\Omega,\ \forall (\mathbf{v}_h, q_h) \in V_h \times Q_h. \quad (26)$$

Therefore, subtracting (2) to (26), the claim follows. □

We now analyze the approximation properties of the proposed finite element space, using the interpolation operator defined in [17]. As shown in [17], it enjoys the following approximation and stability properties:

Lemma 3.6. *The interpolation operator defined as in [17], namely* $R_h : H^s(\Omega) \rightarrow V_{h,0}$*, is such that*

$$\|(\mathbf{v} - R_h^*\mathbf{v}, p - R_h^* p)\|_{\Omega^+}^2 \leq h^2 \left(C_u \|\mu_{max}^{1/2}\mathbf{v}\|_{2,\Omega}^2 + C_p \|p\|_{1,\Omega^+,\mu}^2 \right)\ (\textit{approximation}), \quad (27)$$

$$\|R_h w\|_{r,\Omega} \leq C\|w\|_{s,\Omega},\ 0 \leq r \leq \min(1,s),\ \forall w \in H^s(\Omega)\ (\textit{stability}). \quad (28)$$

Starting from these results, we prove the following theorem.

Theorem 3.7. *The following error estimate holds true*

$$\|(\mathbf{u} - \mathbf{u}_h, p - p_h)\|_{\Omega^+} \leq Ch \left(\|\mu_{max}^{1/2}\mathbf{u}\|_{2,\Omega} + \|p\|_{1,\Omega^+,\mu} \right). \quad (29)$$

Proof. . We have

$$\|(\mathbf{u} - \mathbf{u}_h, p - p_h)\|_{\Omega^+} \leq \|(\mathbf{u} - R_h^*\mathbf{u}, p - R_h^* p)\|_{\Omega^+} + \|(R_h^*\mathbf{u} - \mathbf{u}_h, R_h^* p - p_h)\|_{\Omega^+}.$$

The first term can be estimated directly using the interpolation error estimate (27),

$$\|(\mathbf{u} - R_h^*\mathbf{u}, p - R_h^* p)\|_{\Omega^+} \leq Ch \left(\|\mu_{max}^{1/2}\mathbf{u}\|_{2,\Omega} + \|p\|_{1,\Omega^+,\mu} \right).$$

To estimate the second term we use the *inf-sup* condition (10), to get

$$\begin{aligned}\|(R_h^*\mathbf{u} - \mathbf{u}_h, R_h^* p - p_h)\|_{\Omega^+} \leq \sup_{\mathbf{v}_h, q_h \neq 0} & C_s^{-1}(\mathcal{B}_h[(R_h^*\mathbf{u} - \mathbf{u}_h, R_h^* p - p_h), (\mathbf{v}_h, q_h)] \\ & + c_h(R_h^* p - p_h, q_h) + s_h(R_h^* p - p_h, q_h))/\|(\mathbf{v}_h, q_h)\|_{\Omega^+}.\end{aligned}$$

Adding and subtracting the exact solutions $\mathbf{u}$ and p to $\mathcal{B}_h$ and using the consistency relation for the finite element formulation (25), we get

$$\begin{aligned}\|(R_h^*\mathbf{u} - \mathbf{u}_h, R_h^* p - p_h)\|_{\Omega^+} \leq \sup_{\mathbf{v}_h, q_h \neq 0} & C_s^{-1}(\mathcal{B}_h[(\mathbf{u} - R_h^*\mathbf{u}, p - R_h^* p), (\mathbf{v}_h, q_h)] \\ & + c_h(R_h^* p, q_h) + s_h(R_h^* p, q_h))/\|(\mathbf{v}_h, q_h)\|_{\Omega^+}.\end{aligned}$$

Since the stabilization terms are symmetric we can use the Cauchy-Schwarz inequality followed by the continuity property (14) to get

$$c_h(R_h^* p, q_h) \le c_h(R_h^* p, R_h^* p)^{1/2} c_h(q_h, q_h)^{1/2} \le c_h(R_h^* p, R_h^* p)^{1/2} \|(\mathbf{v}_h, q_h)\|.$$

$$s_h(R_h^* p, q_h) \le s_h(R_h^* p, R_h^* p)^{1/2} s_h(q_h, q_h)^{1/2} \le s_h(R_h^* p, R_h^* p)^{1/2} \|(\mathbf{v}_h, q_h)\|.$$

Finally, using the continuity of $\mathcal{B}_h[(\cdot,\cdot),(\cdot,\cdot)]$, (16), it follows that

$$\begin{aligned}\|(R_h^* \mathbf{u} - \mathbf{u}_h, R_h^* p - p_h)\|_{\Omega^+} \le C\,(&\|(\mathbf{u} - R_h^* \mathbf{u}, p - R_h^* p)\|_{\Omega^+} \\ &+ c_h(R_h^* p, R_h^* p)^{1/2} + s_h(R_h^* p, R_h^* p)^{1/2}\Big).\end{aligned}$$

The first term is estimated using the interpolation error estimate (27), then using the definition of the stabilization terms and the stability properties of the interpolation operator, (28), we have

$$c_h(R_h^* p, R_h^* p) \le C h^2 \sum_{i=1}^{2} \|p_i\|^2_{1,\Omega_i^+,\mu}, \qquad s_h(R_h^* p, R_h^* p) \le C h^2 \sum_{i=1}^{2} \|p_i\|^2_{1,\Omega_i^+,\mu}.$$

Combining the previous estimates, the thesis follows. □

3.3 Conditioning of the pressure matrix

We are now interested in analyzing the conditioning of the system and in particular we focus on the pressure matrix. The forthcoming results will enable us to solve the discrete problem using the classical methods for saddle point problems. In particular, it shows that the Uzawa method [13] can be successfully applied. The discrete problem (2), can be written in algebraic form:

$$\begin{bmatrix} A & B^T \\ -B & S \end{bmatrix} \begin{bmatrix} u \\ p \end{bmatrix} = \begin{bmatrix} f_u \\ f_p \end{bmatrix}$$

where blocks are related to the bilinear forms as follows,

$$a_h(\mathbf{u}_h, \mathbf{v}_h) = (\mathbf{v}_h, A\mathbf{u}_h), \quad b_h(\mathbf{u}_h, q_h) = (q_h, B\mathbf{u}_h),$$

and for the stabilization terms we have $S = S_1 + S_2$ where,

$$c_h(p_h, q_h) = (q_h, S_1 p_h), \quad s_h(p_h, q_h) = (q_h, S_2 p_h).$$

The Schur complement $\mathcal{C}$ is defined as:

$$\mathcal{C} = B A^{-1} B^T + S$$

From (2), we define the following bilinear form:

$$\mathcal{L}_h\left[(\mathbf{u}_h, p_h), (\mathbf{v}_h, q_h)\right] = a_h(\mathbf{u}_h, \mathbf{v}_h) + b_h(\mathbf{v}_h, p_h) - b_h(\mathbf{u}_h, q_h) + c_h(p_h, q_h) + s_h(p_h, q_h) \tag{30}$$

We state the following assumptions:

Assumption 4. *There exist positive numbers $C_a, C_b, C_{s1}, C_{s2}, C_B, \underline{\gamma}, \bar{\gamma}$, independent of $\mathbf{u}_h, \mathbf{v}_h, p_h, q_h$ such that*

$$C_a |||\mathbf{v}_h|||^2 \leq a_h(\mathbf{v}_h, \mathbf{v}_h), \tag{31}$$

$$C_b(1+C)\|p_h\|_{0,\Omega^+,\mu} |||\mathbf{v}_h||| \geq b_h(\mathbf{v}_h, p_h), \tag{32}$$

$$C_{s1}\|p_h\|_{0,\Omega^+,\mu}\|q_h\|_{0,\Omega^+,\mu} \geq c_h(p_h, q_h), \tag{33}$$

$$C_{s2}\|p_h\|_{0,\Omega^+,\mu}\|q_h\|_{0,\Omega^+,\mu} \geq s_h(p_h, q_h), \tag{34}$$

$$C_B\|(\mathbf{u}_h, p_h)\|_{\Omega^+}\|(\mathbf{v}_h, q_h)\|_{\Omega^+} \geq \mathcal{B}_h[(\mathbf{u}_h, p_h), (\mathbf{v}_h, q_h)], \tag{35}$$

$$\underline{\gamma}\|(\mathbf{u}_h, p_h)\|_{\Omega^+} \leq \sup_{\mathbf{v}_h, q_h \neq 0} \frac{\mathcal{L}_h\left[(\mathbf{u}_h, p_h), (\mathbf{v}_h, q_h)\right]}{\|(\mathbf{v}_h, q_h)\|_{\Omega^+}}, \tag{36}$$

$$\bar{\gamma}\|(\mathbf{u}_h, p_h)\|_{\Omega^+} \geq \sup_{\mathbf{v}_h, q_h \neq 0} \frac{\mathcal{L}_h\left[(\mathbf{u}_h, p_h), (\mathbf{v}_h, q_h)\right]}{\|(\mathbf{v}_h, q_h)\|_{\Omega^+}}, \tag{37}$$

Analogously, there exist $\bar{\gamma}' \leq \bar{\gamma}$ such that

$$\bar{\gamma}'\|(\mathbf{u}_h, p_h)\|_{\Omega^+} \geq \sup_{\mathbf{v}_h, q_h \neq 0} \frac{b_h(\mathbf{u}_h, q_h) - c_h(p_h, q_h) - s_h(p_h, q_h)}{\|q\|_{0,\Omega^+,\mu}}. \tag{38}$$

We remark that the existence of $\bar{\gamma}'$ follows from (37) with $\bar{\gamma}' = \bar{\gamma}$. However, we can consider the case in which a better estimate of $\bar{\gamma}'$ may be available. Inequalities (31), (32), (33), (34) and (35) correspond to results of Lemma 3.2 and (36) is the thesis of theorem 3.1. All these inequalities have been previously proved. In particular, the discrete norm equivalence (7) has been used in (13) to write (32). Inequality (37) follows from the assumptions (33), (34) and (35).

Theorem 3.8. *Under the assumption 4, the eigenvalues of $\mathcal{C}$ are localized as follows:*

$$\lambda_n(\mathcal{C}) \in \left\{ z \in \mathbb{C} : \underline{\gamma} \leq |z| \leq \bar{\gamma}'\sqrt{1 + \left(\frac{C_b(1+C)}{C_a}\right)^2} \right\}. \tag{39}$$

Proof. To prove (39), we follow the general framework proposed in [10]. For each $p_h \in Q_h$, let $\tilde{\mathbf{u}}_h \in V_h$ be defined by

$$a_h(\tilde{\mathbf{u}}_h, \mathbf{v}_h) + b_h(\mathbf{v}_h, p_h) = 0 \quad \forall \mathbf{v}_h \in V, \quad \text{that is,} \quad \tilde{\mathbf{u}}_h = -A^{-1}B^T p_h. \tag{40}$$

Taking $\mathbf{u}_h = \tilde{\mathbf{u}}_h$ in (30), makes $\mathcal{L}_h\left[(\mathbf{u}_h, p_h), (\mathbf{v}_h, q_h)\right] = c_h(p_h, q_h) + s_h(p_h, q_h) - b_h(\mathbf{u}_h, q_h) = (q_h, \mathcal{C}p_h)$ independent of $\mathbf{v}_h$; hence, using (36) and (38),

$$\underline{\gamma}\|(\tilde{\mathbf{u}}_h, p_h)\|_{\Omega^+} \leq \sup_{\mathbf{v}_h, q_h \neq 0} \frac{(q_h, \mathcal{C}p_h)}{\|(\mathbf{v}_h, q_h)\|_{\Omega^+}} \leq \sup_{q_h \neq 0} \frac{(q_h, \mathcal{C}p_h)}{\|q_h\|_{0,\Omega^+,\mu}} \leq \bar{\gamma}'\|(\tilde{\mathbf{u}}_h, p_h)\|_{\Omega^+}. \tag{41}$$

From (40), (31) and (32) we have,

$$C_a|||\tilde{\mathbf{u}}_h|||^2 \leq a_h(\tilde{\mathbf{u}}_h, \tilde{\mathbf{u}}_h) = -b_h(\tilde{\mathbf{u}}_h, p_h) \leq C_b(1+C)\|p_h\|_{0,\Omega^+,\mu}|||\tilde{\mathbf{u}}_h|||,$$

so that $|||\tilde{\mathbf{u}}_h||| \leq \frac{C_b}{C_a}\|p_h\|_{\Omega^+}$, yielding the following estimate,

$$\|p_h\|_{0,\Omega^+,\mu} \leq \|(\tilde{\mathbf{u}}_h, p_h)\|_{\Omega^+} \leq \sqrt{1 + \left(\frac{C_b(1+C)}{C_a}\right)^2}\|p_h\|_{0,\Omega^+,\mu},$$

and equation (41) becomes

$$\underline{\gamma}\|p_h\|_{0,\Omega^+,\mu} \leq \sup_{q_h \neq 0} \frac{(q_h, \mathcal{C}p_h)}{\|q_h\|_{0,\Omega^+,\mu}} \leq \bar{\gamma}' \sqrt{1 + \left(\frac{C_b(1+C)}{C_a}\right)^2} \|p_h\|_{0,\Omega^+,\mu}.$$

□

4 Numerical results

We analyse the order of convergence of two variants of the proposed method compared with two reference methods and we investigate how Brezzi-Pitkaranta stabilization improves the conditioning of the algebraic problem.

4.1 Comparison of different variants of methods

The previous analysis is valid for those choices of finite element spaces and stabilization terms for which the *inf-sup* condition is guaranteed on the restricted sub-domains. The stabilization on the *extended cut region* makes the *inf-sup* condition to be globally satisfied. We analyze the numerical performances of the following combination:

- $\mathbb{P}^1_b - \mathbb{P}^1$ elements with Brezzi-Pitkaranta stabilization on the cut region. We notice that, since the *inf-sup* condition is satisfied because of the bubble stabilization, we do not need the additional term $c_h(p_h, q_h)$.
- $\mathbb{P}^1 - \mathbb{P}^1$ with Brezzi-Pitkaranta stabilization on all the domain, i.e. both $c_h(p_h, q_h)$ and $s_h(p_h, q_h)$ are active.

These two choices will be compared with two *reference methods*. The first one employs $\mathbb{P}^1_b - \mathbb{P}^1$ elements without any additional stabilization in the *extended cut region* ($s_h(p_h, q_h) = 0$). It is the method where we observed instabilities in the pressure approximation, shown in Figure 1. The second one has been proposed by Burman-Becker-Hansbo [3] and it consists in choosing $\mathbb{P}^1 - \mathbb{P}^0$ elements with a stabilization based on the jump of the pressure along the edges of the mesh, so we define:

$$c_h(p_h, q_h) + s(p_h, q_h) := \sum_{F \in \mathcal{F}_1} \int_F \frac{\gamma_p}{\mu_1} h_F [\![p_{h,1}]\!] [\![q_{h,1}]\!] ds + \sum_{F \in \mathcal{F}_2} \int_F \frac{\gamma_p}{\mu_2} h_F [\![p_{h,2}]\!] [\![q_{h,2}]\!] ds, \tag{42}$$

where $\mathcal{F}_i$ denotes the set of interior faces of $\mathcal{T}^+_{h,i}$.

From the standpoint of accuracy, the considered methods are substantially equivalent. Indeed, they all satisfy the following theoretical estimate [11, 19]:

$$\|\mathbf{u} - \mathbf{u}_h\|_{1,\Omega,\mu} + \|p - p_h\|_{0,\Omega^+,\mu} \leq Ch(\|\mathbf{u}\|_{2,\Omega} + \|p\|_{1,\Omega}) \tag{43}$$

In what follows we will show that the performance of all methods is coherent to the theory, but appreciable differences may appear in the magnitude of the error.

A strong point in favor of the Brezzi-Pitkaranta stabilization is that it is easy to implement, that is it keeps to a minimum the effort needed to introduce the stabilization term in a pre-existing finite element code. Moreover, it can be easily used in a parallel context. In contrast, the assembling of a stabilization term that needs integration on the edges of the elements, such as the Burman-Becker and Hansbo stabilization, usually requires to access information about the adjacent elements to each edge, which increases the communication between processors.

4.2 Test cases and results

The numerical tests have been implemented in the C++ finite element library `LifeV` (`www.lifev.org`), developed by the collaboration between four institutions: École Polytechnique Fédérale de Lausanne (CMCS), Politecnico di Milano (MOX), INRIA (REO, ESTIME) and Emory University.

We solve the saddle point problems in the domain $\Omega = [0,1]^2$ crossed by the interface $\Gamma = \{x, y | (x-x_c)^2 + (y-y_c)^2 = a^2\}$. We set $a = 0.25$ and $x_c = y_c = 0.5$. Let us define $\Omega_1 = \{x, y | (x-x_c)^2 + (y-y_c)^2 < a^2\}$ the internal part of the domain with respect to the orientation of the normal of Γ, and Ω_2 is the external part. We set $\gamma_s = 1$ and the penalty parameters $\gamma_p = \gamma_u = 10$.

We consider three different test cases. In the first two tests there is no variation in the parameters of the problem between the two sides of the interface. The surface Γ is then an *artificial* interface, however the additional XFEM degrees of freedom and the weak imposition of the conditions across the surface can produce extra numerical errors in the region near the interface. We discuss in details the convergence analysis for the error on the velocity and pressure solution.

Test 1: Poiseuille's flow We start from the Poiseuille's flow in the domain Ω crossed by Γ, for the verification of the numerical solver. We remind that in a Poiseuille's flow, the velocity profile is parabolic for the horizontal component and null for the vertical one. The gradient of the pressure is linear. As we can see in Figure 5, the numerical results are coherent with the theoretical estimates (43).

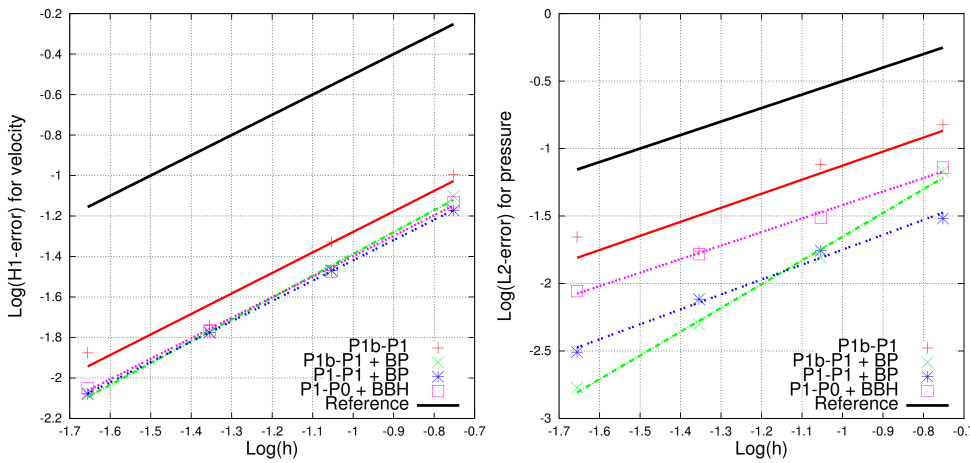

(a) H^1-norm error for velocity (b) L^2-norm error for pressure

Figure 5: Convergence analysis for test 1

Test 2: An artificial interface in an incompressible medium We analyse the case of an artificial interface in an incompressible fluid with constant material properties over the entire domain. For problem 1, the following analytical solution is available:

$$\mathbf{u}(x,y) = \begin{cases} 20xy^3 \\ 5x^4 - 5y^4 \end{cases}$$
$$p(x,y) = 60x^2y - 20y^3 - 5.$$

We observe that the velocity approximation error is very similar for the four considered methods. For the approximation of the pressure, methods based on the Brezzi-Pitkaranta stabilization on the cut region perform slightly better that the others.

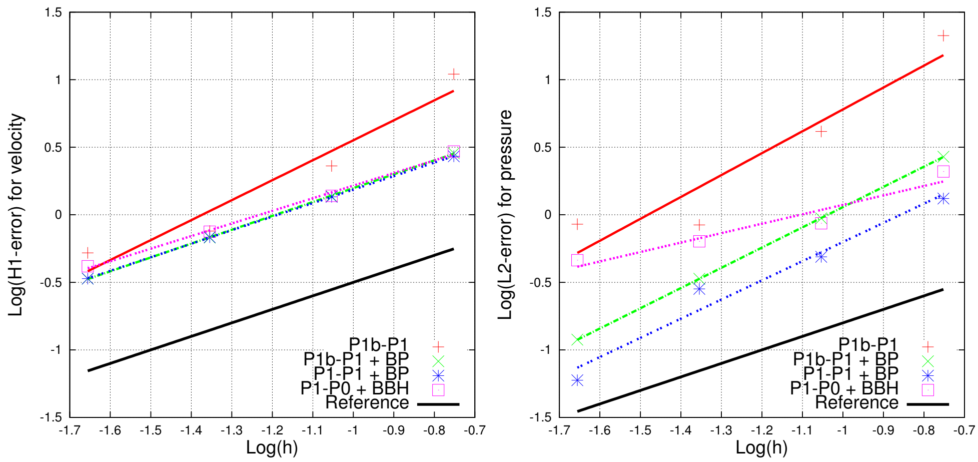

(a) H^1-norm error for velocity (b) L^2-norm error for pressure

Figure 6: Convergence analysis for test 2

Test 3: An elastic interface problem After these preliminary tests, we analyze a problem with heterogeneous coefficients [3]. This is an incompressible linear elastic problem that can be reinterpreted as a Stokes flow with suitable forcing terms. More precisely, we set $E_1 = E_2 = 1$, $\nu_2 = 0.25$ and $\nu_1 = 0.49$. Coefficients μ_i are defined as follows: $\mu_i = E_i/(2(1+\nu_i))$. Using polar coordinates, where $r = \sqrt{(x-x_c)^2 + (y-y_c)^2}$, $b = 0.5$, the analytical solution for velocity and pressure are given by the following expressions, for $\nu_1 \neq 0.5$:

$$u_r(r,\theta) = \begin{cases} c_1 r & \text{in } \Omega_1 \\ (r - \frac{b^2}{r})c_2 + \frac{b^2}{r} & \text{in } \Omega_2 \end{cases}$$
$$u_\theta(r,\theta) = 0$$
$$p(r,\theta) = \begin{cases} -2c_1\lambda_1 & \text{in } \Omega_1 \\ -2c_2\lambda & \text{in } \Omega_2 \end{cases}$$

$$c_1 = \left(1 - \frac{b^2}{a^2}\right) c_2 + \frac{b^2}{a^2}$$

$$c_2 = \frac{(\lambda_1 + \mu_1 + \mu_2)b^2}{(\lambda_2 + \mu_2)a^2 + (\lambda_1 + \mu_1)(b^2 - a^2) + \mu_2 b^2}.$$

We notice that the variation on the Poisson coefficient produces a kink in the radial velocity profile and a strong discontinuity in the pressure solution. Strictly speaking, p can be interpreted as the pressure only in the incompressible case (Stokes problem), but we shall omit this distinction. Similarly to the previous results, performances of the methods are quite similar concerning the velocity approximation. In the approximation of the pressure, Figure 7 shows that using the Brezzi-Pitkaranta stabilization for $\mathbb{P}^1_b - \mathbb{P}^1$ and $\mathbb{P}^1 - \mathbb{P}^1$ elements we obtain a smaller error with respect to the case of the mini-elements and stabilized $\mathbb{P}^1 - \mathbb{P}^0$. In particular, the best performances in terms of approximation error are observed for equal order $\mathbb{P}^1 - \mathbb{P}^1$ elements with Brezzi-Pitkaranta stabilization. Finally, we were interested in studying the behavior of the scheme for two different choices of the weights k_i. These results are obtained using the weights defined in (3). In Figure 8, we perform the same test using the weights defined in [16], which do not account for the heterogeneity of viscosity. Comparing the results reported in Figure 7 and 8, we do not observe a significant difference in the numerical solution. We remark that the computational cost of these weights is very similar and we conclude that both the choices are suitable to solve a problem with a mild heterogeneity between coefficients.

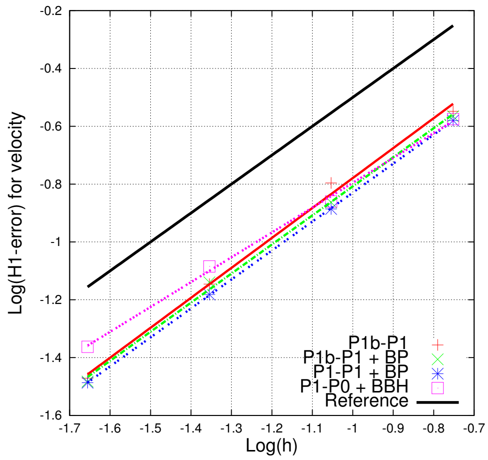

(a) H^1-norm error for velocity

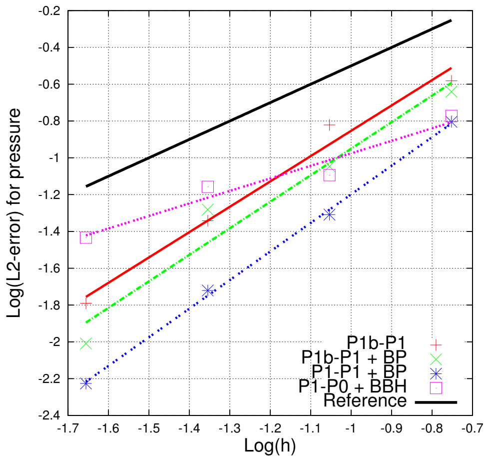

(b) L^2-norm error for pressure

Figure 7: Convergence analysis for test 3, using the averaging weights defined in (3).

4.3 Problem conditioning

As we already pointed out, the Nitsche-XFEM method allows for using meshes independent on the position of Γ, but instabilities in the *cut region* depend on how the interface crosses the elements. For this reason, we study the conditioning of the pressure Schur complement matrix $\mathcal{C}$ for the third test case previously presented and we use the $\mathbb{P}^1 - \mathbb{P}^1$ elements with Brezzi-Pitkaranta

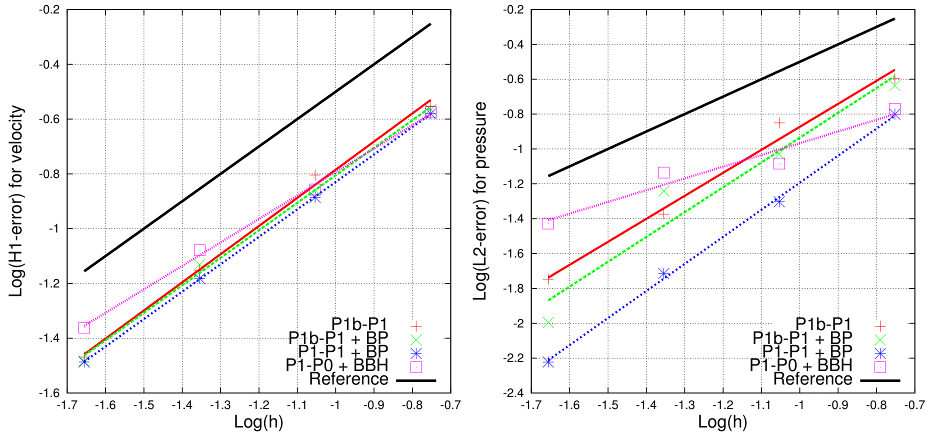

(a) H^1-norm error for velocity (b) L^2-norm error for pressure

Figure 8: Convergence analysis for test 3, using the averaging weights defined in [16].

stabilization. By increasing the radius of the circular interface Γ, see Figure 1, we modify the intersections between the mesh and the interface. According to the theory, we expect the method proposed is not influenced by the geometry of the problem . The estimate of the conditioning number is done following [18].

In table 1, we collect the obtained results. First of all, we observe that the conditioning of the matrix $\mathcal{C}$ is almost constant when using $\mathbb{P}^1 - \mathbb{P}^1$ elements with Brezzi-Pitkaranta stabilization on all the domain, as expected from (39). That estimate is independent on how the interface cuts the mesh. Following the lines of [25], we compare the conditioning of the pressure matrix with the mass matrix $\mathcal{M}_p^+$ defined below:

$$[\mathcal{M}_p^+]_{mn} = \sum_{i=1}^{2} \int_{\Omega_i^+} q_h^m q_h^n dx, \qquad q_h^m, q_h^n \in Q_h,$$

where we remark that the integrals of basis functions having support in a $K \in \mathcal{G}_h$ are computed on the entire element K. Consequently, this matrix differs from the mass matrix computed following the XFEM approach:

$$[\mathcal{M}_p]_{mn} = \sum_{i=1}^{2} \int_{\Omega_i} q_h^m q_h^n dx, \qquad q_h^m, q_h^n \in Q_h.$$

The Nitsche-XFEM method with stabilization is robust. Indeed, the eigenvalues of $\mathcal{C}$ are bounded by the eigenvalues of $\mathcal{M}_p^+$. Without stabilization, mini-elements are ill conditioned. Indeed (39) does not hold true in this case. More precisely, in this case the smallest eigenvalue of the Schur complement depends on the size of the smallest cut element. This behavior is also observed for the mass matrix $\mathcal{M}_p$. The Brezzi-Pitkaranta stabilization makes $\underline{\gamma}$ independent on the cut-element size and thus it prevents the minimum eigenvalue of A from approaching zero (i.e. the spectrum of this matrix is similar to $\mathcal{M}_p^+$).

Interface Radius	$\kappa(\mathcal{C})$ $\mathbb{P}^1_{bubble} - \mathbb{P}^1$	$\kappa(\mathcal{C})$ $\mathbb{P}^1 - \mathbb{P}^1$ + BP stab.	$\kappa(\mathcal{M}_p)$
0.250	$2.15 \cdot 10^3$	139.44	223.92
0.270	$2.36 \cdot 10^4$	119.24	786.44
0.280	$1.57 \cdot 10^6$	115.66	$1.34 \cdot 10^4$
0.285	$5.48 \cdot 10^7$	113.32	$6.3 \cdot 10^6$

Table 1: Conditioning of the Schur complement $\mathcal{C}$ for small perturbations of the radius of Ω_1 and conditioning of the pressure mass matrix $\mathcal{M}_p$ ($h_K = 0.1423$). The latter has to be compared with the condition number of $\mathcal{M}_p^+$ that is 24.68.

5 Conclusions

This work arises from the observation that the approximation of saddle point problems with extended finite elements poses some stability issues. In particular, for Stokes problem the approximation of the pressure may be locally unstable. Standard mixed finite element spaces combined with simple enrichment strategies lead to a satisfactory approximation method, provided that pressure stabilization is introduced into the scheme. The general framework of symmetric stabilization techniques is suitable to cure this kind of issues. In particular, we have shown that the Brezzi-Pitkaranta stabilization scheme is effective also in this new approximation context. The algebraic properties of the scheme are also analyzed, enabling the application of standard solvers, such as the Uzawa method.

Acknowledgements

This project was supported by the ERC Advanced Grant N.227058 MATHCARD and by Politecnico di Milano through the grant ”5/1000 Junior - Computational models for heterogeneous media” CUP D41J10000490001. The second and fourth authors also acknowledge the support of the Italian MIUR through PRIN09 project n. 2009Y4RC3B 001. The authors would also like acknowledge Dr. Alessio Fumagalli and Dr. Antonio Cervone for many fruitful discussion on the implementation of the original code in `LifeV`.

References

[1] C. Annavarapu, M. Hautefeuille, and J.E. Dolbow. A robust Nitsche's formulation for interface problems. *Computer Methods in Applied Mechanics and Engineering*, 225-228:44–54, 2012.

[2] R.F. Ausas, G.C. Buscaglia, and S.R. Idelsohn. A new enrichment space for the treatment of discontinuous pressures in multi-fluid flows. *International Journal for Numerical Methods in Fluids*, 70(7):829–850, 2012.

[3] R. Becker, E. Burman, and P. Hansbo. A Nitsche extended finite element method for incompressible elasticity with discontinuous modulus of elas-

ticity. *Computer Methods in Applied Mechanics and Engineering*, 198(41-44):3352–3360, 2009.

[4] F. Brezzi and M. Fortin. *Mixed and hybrid finite element methods*, volume 15 of *Springer Series in Computational Mathematics*. Springer-Verlag, New York, 1991.

[5] F. Brezzi and J. Pitkäranta. On the stabilization of finite element approximations of the Stokes equations. In *Efficient solutions of elliptic systems (Kiel, 1984)*, volume 10 of *Notes Numer. Fluid Mech.*, pages 11–19. Vieweg, Braunschweig, 1984.

[6] E. Burman. Ghost penalty [la pénalisation fantôme]. *Comptes Rendus Mathematique*, 348(21-22):1217–1220, 2010.

[7] E. Burman and P. Hansbo. Fictitious domain methods using cut elements : Iii. a stabilized Nitsche method for Stokes' problem. Technical Report 2011:06, School of Engineering, Jönköping University, JTH, Mechanical Engineering, 2011.

[8] E. Burman and P. Hansbo. Fictitious domain finite element methods using cut elements: Ii. a stabilized Nitsche method. *Applied Numerical Mathematics*, 62(4):328–341, 2012.

[9] G.C. Buscaglia and A. Agouzal. Interpolation estimate for a finite-element space with embedded discontinuities. *IMA Journal of Numerical Analysis*, 32(2):672–686, 2012.

[10] C. D'Angelo and P. Zunino. Robust numerical approximation of coupled Stokes' and Darcy's flows applied to vascular hemodynamics and biochemical transport. *ESAIM: Mathematical Modelling and Numerical Analysis*, 45(3):447–476, 2011.

[11] A. Ern and J. Guermond. *Theory and practice of finite elements*, volume 159 of *Applied Mathematical Sciences*. Springer-Verlag, New York, 2004.

[12] T.-P. Fries and T. Belytschko. The extended/generalized finite element method: An overview of the method and its applications. *International Journal for Numerical Methods in Engineering*, 84(3):253–304, 2010.

[13] V. Girault and P. Raviart. *Finite element methods for Navier-Stokes equations*, volume 5 of *Springer Series in Computational Mathematics*. Springer-Verlag, Berlin, 1986. Theory and algorithms.

[14] S. Gross and A. Reusken. *Numerical methods for two-phase incompressible flows*, volume 40 of *Springer Series in Computational Mathematics*. Springer-Verlag, Berlin, 2011.

[15] S. Groß and A. Reusken. An extended pressure finite element space for two-phase incompressible flows with surface tension. *Journal of Computational Physics*, 224(1):40–58, 2007.

[16] A. Hansbo and P. Hansbo. An unfitted finite element method, based on Nitsche's method, for elliptic interface problems. *Computer Methods in Applied Mechanics and Engineering*, 191(47-48):5537–5552, 2002.

[17] P. Hansbo, M. G Larson, and S. Zahedi. A Nitsche method for a Stokes interface problem. *arXiv preprint arXiv:1205.5684*, 2012.

[18] N.J. Higham and F. Tisseur. A block algorithm for matrix 1-norm estimation, with an application to 1-norm pseudospectra. *SIAM Journal on Matrix Analysis and Applications*, 21(4):1185–1201, 2000.

[19] A. Quarteroni and A. Valli. *Numerical Approximation of Partial Differential Equations*. Springer-Verlag, Berlin, Heidelberg, New York, 1994.

[20] A. Reusken. Analysis of an extended pressure finite element space for two-phase incompressible flows. *Comput. Vis. Sci.*, 11(4-6):293–305, 2008.

[21] H. Sauerland and T.-P. Fries. The extended finite element method for two-phase and free-surface flows: A systematic study. *Journal of Computational Physics*, 230(9):3369–3390, 2011.

[22] F.S. Sousa, R.F. Ausas, and G.C. Buscaglia. Numerical assessment of stability of interface discontinuous finite element pressure spaces. *Computer Methods in Applied Mechanics and Engineering*, 245-246:63–74, 2012.

[23] A. Zilian and H. Netuzhylov. Hybridized enriched space-time finite element method for analysis of thin-walled structures immersed in generalized newtonian fluids. *Computers and Structures*, 88(21-22):1265–1277, 2010.

[24] P. Zunino. Analysis of backward euler/extended finite element discretization of parabolic problems with moving interfaces. *Computer Methods in Applied Mechanics and Engineering*, 258:152–165, 2013.

[25] P. Zunino, L. Cattaneo, and C.M. Colciago. An unfitted interface penalty method for the numerical approximation of contrast problems. *Applied Numerical Mathematics*, 61(10):1059–1076, 2011.

MOX Technical Reports, last issues

Dipartimento di Matematica "F. Brioschi",
Politecnico di Milano, Via Bonardi 9 - 20133 Milano (Italy)

32/2013 Taddei, T.; Perotto, S.; Quarteroni, A.
Reduced basis techniques for nonlinear conservation laws

31/2013 Dassi, F.; Ettinger, B.; Perotto, S.; Sangalli, L.M.
A mesh simplification strategy for a spatial regression analysis over the cortical surface of the brain

30/2013 Cagnoni, D.; Agostini, F.; Christen, T.; de Falco, C.; Parolini, N.; Stevanović, I.
Multiphysics simulation of corona discharge induced ionic wind

29/2013 Lassila, T.; Manzoni, A.; Quarteroni, A.; Rozza, G.
Model order reduction in fluid dynamics: challenges and perspectives

28/2013 Ekin, T.; Ieva, F.; Ruggeri, F.; Soyer, R.
Statistical Issues in Medical Fraud Assessment

27/2013 Tagliabue, A.; Dede', L.; Quarteroni, A.
Isogeometric Analysis and Error Estimates for High Order Partial Differential Equations in Fluid Dynamics

24/2013 Mazzieri, I.; Stupazzini, M.; Guidotti, R.; Smerzini, C.
SPEED-SPectral Elements in Elastodynamics with Discontinuous Galerkin: a non-conforming approach for 3D multi-scale problems

25/2013 Cattaneo, Laura; Zunino, Paolo
Computational models for coupling tissue perfusion and microcirculation

26/2013 Ieva, F.; Paganoni, A.M.
Detecting and visualizing outliers in provider profiling via funnel plots and mixed effect models

23/2013 Srensen, H.; Goldsmith, J.; Sangalli, L.M.
An introduction with medical applications to functional data analysis